Received: 3 December 2019 | Revised: 22 February 2020 | Accepted: 15 March 2020

DOI: 10.1002/jnr.24622

RESEARCH ARTICLE

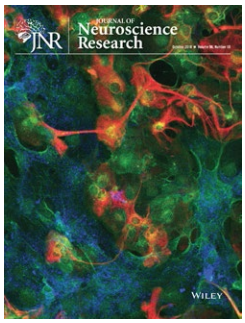

Quantitative proteomic profiling of the rat substantia nigra places glial fibrillary acidic protein at the hub of proteins dysregulated during aging: Implications for idiopathic Parkinson's disease

Yolanda Gómez-Gálvez[1,2] | Heidi R. Fuller[1,3] | Silvia Synowsky[4] | Sally L. Shirran[4] | Monte A. Gates[1,2]

[1]School of Pharmacy and Bioengineering, Keele University, Keele, UK

[2]School of Medicine, Keele University, Keele, UK

[3]Wolfson Centre for Inherited Neuromuscular Disease, RJAH Orthopaedic Hospital, Oswestry, UK

[4]BSRC Mass Spectrometry and Proteomics Facility, University of St Andrews, Fife, UK

Correspondence
Monte A. Gates and Heidi R. Fuller, School of Pharmacy and Bioengineering, Keele University, Keele, Staffordshire, UK.
Email: m.a.gates@keele.ac.uk (M. A. G.) and h.r.fuller@keele.ac.uk (H. R. F.)

Funding information
Keele University ACRORN funding scheme; Keele University School of Medicine

Abstract

There is a strong correlation between aging and onset of idiopathic Parkinson's disease, but little is known about whether cellular changes occur during normal aging that may explain this association. Here, proteomic and bioinformatic analysis was conducted on the substantia nigra (SN) of rats at four stages of life to identify and quantify protein changes throughout aging. This analysis revealed that proteins associated with cell adhesion, protein aggregation and oxidation-reduction are dysregulated as early as middle age in rats. Glial fibrillary acidic protein (GFAP) was identified as a network hub connecting the greatest number of proteins altered during aging. Furthermore, the isoform of GFAP expressed in the SN varied throughout life. However, the expression levels of the rate-limiting enzyme for dopamine production, tyrosine hydroxylase (TH), were maintained even in the oldest animals, despite a reduction in the number of dopamine neurons in the SN pars compact(SNc) as aging progressed. This age-related increase in TH expression per neuron would likely to increase the vulnerability of neurons, since increased dopamine production would be an additional source of oxidative stress. This, in turn, would place a high demand on support systems from local astrocytes, which themselves show protein changes that could affect their functionality. Taken together, this study highlights key processes that are altered with age in the rat SN, each of which converges upon GFAP. These findings offer insight into the relationship between aging and increased challenges to neuronal viability, and indicate an important role for glial cells in the aging process.

Edited by Sheila Fleming.

The peer review history for this article is available at https://publons.com/publon/10.1002/jnr.24622.

KEYWORDS

aging, dopaminergic neuron, glial fibrillary acidic protein, proteome, proteomics, RRID:AB_11145309, RRID:AB_2109791, RRID:AB_228307, RRID:AB_228341, RRID:AB_2336820, RRID:AB_2631098, RRID:AB_390204, RRID:MGI:5651135, RRID:SCR_001881, RRID:SCR_002798, RRID:SCR_003070, RRID:SCR_004946, RRID:SCR_005223, substantia nigra

1 | INTRODUCTION

There is an inextricable link between aging and idiopathic Parkinson's disease (iPD). The typical onset of iPD is just after 60 years of age (Hindle, 2010), and there is a 10-fold increase in the occurrence of the disease between the ages of 50 and 80 (Van Den Eeden et al., 2003). Although aging is most certainly a risk factor, very little is known about whether changes occur in the region of the brain affected by iPD (i.e., the substantia nigra SNc) during normal aging that might make resident dopamine neurons there more susceptible to neurodegeneration.

What is known, however, is that there is a direct correlation between normal aging of the brain and an increased expression of markers of neurodegenerative conditions (Collier, Kanaan, & Kordower, 2011). A comparison of the proteome of healthy young and old humans, for example, found that proteins normally associated with Alzheimer's disease (AD) were increased in expression in the orbitofrontal cortex as aging progressed (Pabba et al., 2017). In the nigrostriatal system, studies have shown that there is an increased accumulation of alpha-synuclein in SNc dopamine neurons during normal aging (Chu & Kordower, 2007; Naskar, Mahadevan, Philip, & Alladi, 2019), and that ubiquitin positive inclusions (Lewy bodies) occur in the region during normal aging of both human and non-human primates (Beach et al., 2004; Siddiqi, Kemper, & Killiany, 1999). What these studies highlight is that even in the absence of a degenerative condition, the proteome of the normal aging brain can be altered in a way that shows similarities to neurodegenerative disease.

At present, however, it is unclear whether the expression of proteins related to neurodegenerative disease in the aging brain are causative factors, or whether they indicate a response by cells to other—or earlier—protein changes. It is becoming increasingly apparent though that the protein profile of all cells (not just the neurons at risk) should be considered when exploring links between aging, protein alterations, and neuronal viability (Walker, 2018). In the seminal work by Peng et al. (2018), for example, aberrant aggregation of the alpha-synuclein protein was shown to occur in oligodendrocytes in several regions of the brain. Differential effects on neuronal viability were observed with distinct conformational "strains" of alpha-synuclein in the aggregate, and the effects were dependent on the particular phenotype of cell and/or region of the brain the protein aggregates occurred within (Peng et al., 2018). When combined with studies from the aging brain, these findings suggest that proteome changes do occur during normal aging, and that changes in either neurons themselves or the cells that surround them could make dopamine neurons in the SNc more susceptible to degeneration.

Significance

Neurodegenerative diseases are associated with aging. However, it is currently unclear what changes during normal aging that makes these diseases more likely. The research conducted here has identified changes that occur during normal aging of the region of the brain that degenerates in Parkinson's disease. This has detailed alterations of a network of proteins, the greatest number of which is associated with one glial fibrillary acidic protein that is found specifically in support cells (glia). These results provide insight into how cells in the brain change during normal aging, and how these changes could lessen the ability of neurons to survive.

Quantitative proteomics technology provides an opportunity to clearly identify and quantify alterations in the expression of individual proteins and pathways in cells and tissues throughout aging. Here, we have used iTRAQ™-based proteomics analysis to quantitatively compare the proteome of the SN of rats at four stages of life to identify age-related changes in protein expression. Bioinformatics analysis of the proteomics data revealed an age-related differential expression of proteins associated with protein aggregation, oxidation-reduction, and astrocyte function. Interestingly, the glial fibrillary acidic protein (GFAP) formed the center of a network of proteins differentially expressed with age. Further analyses revealed that GFAP-delta, an isoform known to negatively affect astrocyte function, was increased in expression in middle-aged rats. This pattern of expression occurred concomitantly with dopamine neurons becoming reduced in number, while increasing in size and maintaining tyrosine hydroxylase (TH) expression levels in the SN. Taken together, these results add to the growing concept of a "pre-parkinsonian" state existing in the SN during aging (Collier et al., 2011; Collier, Kanaan, & Kordower, 2017), and suggests that normal aging may create a protein profile that challenges dopamine neuron viability and contributes to age-related vulnerability to neurodegenerative disease.

2 | MATERIALS AND METHODS

2.1 | Animals

All animal experiments were performed following guidelines established by the Animal Welfare and Ethical Review Body (AWERB) at Keele University and conducted under the licensed authority of the UK Home Office (PPL40/3556). Animals were maintained in a 12/12-hr light/dark cycle at a stable room temperature (RT; 22 ± 1°C), and were given free access to food, water, and environmentally enriching articles.

For the purpose of comparative analyses, male and female Sprague Dawley rats (RRID:MGI:5651135) were grouped into four experimental groups: postnatal day 14 rats (were considered "juvenile"), 8-month-old rats ("young adult"), 16-month-old rats ("middle age"), and 21- to 25-month-old rats ("old").

2.2 | Tissue extraction and preparation

Rats were killed with an overdose of pentobarbitone anesthetic (0.5 ml/100 g) via an intraperitoneal injection, and transcardially perfused with ice-cold sterile 0.9% sodium chloride (saline). Brain specimens were removed rapidly and cut in half along the sagittal midline. The right hemisphere was used for proteomics and Western blotting, while the left hemisphere was kept for immunohistochemistry (IHC) analyses. To obtain protein samples, the SNc region was individually dissected from each right hemibrain after 0.5-mm thick coronal slices were made in the saline-infused specimen. Using the medial terminal nucleus (MTN) of the accessory optic tract as a guide (Winkler, Sauer, Lee, & Björklund, 1996), a region was selected to highly enrich the samples for the SNc region. To exclude tissue from the ventral tegmental area and pars reticulata nuclei, only tissue that was lateral to the MTN and dorsal to the midbrain bulge (representing pars reticulata) was used for proteomics processing. Although it is possible that some adjacent reticulata and/or VTA region could be included in these samples, we refer to the samples simply as "substantia nigra pars compacta" or "SNc" due to their high enrichment of the SNc region and the very close association of the surrounding tissue to the SNc (i.e., adjacent regions which could affect the milieu of the SNc itself). The left hemibrain specimens were fixed by immersion in a 4.0% solution of paraformaldehyde (PFA) in 1× Tris-buffered saline (TBS) overnight, and cryoprotected in a 30% sucrose solution in TBS until "sunk" (saturated) for sectioning.

2.3 | Protein extraction

Four animals per age group (two males and two females) were used for quantitative proteomics analysis and Western blotting. To minimize sample losses due to the small size of SNc tissue, the four samples within each experimental group (juvenile, young adult, middle age, or old) were pooled before protein extraction. Pooled samples of each experimental group were then homogenized in four volumes (w/v) of 6M urea, 2M thiourea, 2% CHAPS, and 0.5% sodium dodecyl sulfate (SDS) using a pellet pestle (Fuller, Hurtado, Wishart, & Gates, 2014). Samples were left on ice for 10 min, followed by a brief sonication. Samples were subsequently left on ice for an additional 10 min, followed by centrifugation at 13,000*g* for 10 min at 4°C. The extracted proteins in the resulting supernatants were precipitated in six volumes of ice-cold acetone overnight at −20°C. The next day, samples were centrifuged at 13,000*g* for 10 min at 4°C, and each pellet resuspended in 200 µl of 500 mM tetraethylammonium bromide (TEAB) in ultrapure water (Chromasolve) for mass spectrometry analysis. For Western blotting, total protein was extracted from individual SNc samples (without pooling) by homogenizing the tissue in 200 µl of cold RIPA buffer (Sigma, #R0278) with Halt™ protease EDTA-free inhibitor cocktail (ThermoFisher Scientific, #87785) using a pellet pestle (20 strokes). Samples were left on ice for 10 min, followed by sonication. Samples were then placed on ice for an additional 10 min and then centrifuged at 13,000*g* for 10 min at 4°C. The protein concentration from each was quantified using a Bradford protein assay (Bradford, 1976).

2.4 | Mass spectrometry analysis

Samples were prepared for mass spectrometry analysis according to the protocol described in the isobaric tags for relative and absolute quantitation (iTRAQ^{TM}) labelling kit (Biotech, 2016; Applied Biosystems, Foster City, CA, USA). Reduction of proteins and blocking of cysteine residues were performed using the reagents and protocol of the iTRAQ^{TM} labelling kit. Proteins were then digested with sequencing grade modified trypsin (5 µg/100 µg of protein, Promega, #V5113) overnight at 37°C, followed by drying in a centrifugal vacuum concentrator to reduce the volume of the sample digest for maximal labeling efficiency. Each tag was incubated with 85 µg of the total protein and any remaining protein extract was kept at −80°C for future Western blotting. Peptides were labeled with 4-plex iTRAQ^{TM} tagging reagents according to the protocol in the iTRAQ^{TM} kit, and were assigned to each sample group as follows: 114-juvenile, 115-young adult, 116-middle age, 117-old.

High pH reverse-phase liquid chromatography (RPLC) fractionation and liquid chromatography-tandem mass spectrometry analysis were conducted as described previously (Šoltić et al., 2019). Briefly, iTRAQ^{TM} labeled peptides were combined into one tube, concentrated using a vacuum concentrator, and then resuspended in 100 µl of 10 mM ammonium formate (NH_4HCO_2), 2% acetonitrile (MeCN), pH 10.0. The peptides were then fractionated by high pH RPLC using a C18 column (XBridge C18 5 µm, 4.6 × 100 mm, Waters) to give 12 fractions. The pooled fractions were concentrated in a vacuum concentrator and resuspended in 30 µl of 0.1% of formic acid (FA).

One third of each fraction containing the labeled peptides was analyzed by mass spectrometry using a TripleTOF 5600+ tandem mass spectrometer (AB Sciex), controlled by Analyst® TF software

(AB Sciex), and coupled to a NANOSpray II source. The raw mass spectrometry data file was analyzed by ProteinPilot software, version 5.0.1.0 (Applied Biosystems) with the Paragon™ database search and Pro Group™ Algorithm using the UniProtKB/Swiss-Prot FASTA database (RRID:SCR_004946). The general Paragon™ search analysis parameters were: type "iTRAQ™ 4plex (Peptide Labeled)", cysteine alkylation "MMTS", digestion "trypsin" as the cleavage enzyme, instrument "TripleTOF", and species "Rattus norvergicus" for sample parameters; processing parameters were specified as "quantitative", "bias correction", "background correction"; "thorough ID" and "biological modifications". Proteins that showed a protein threshold >5 were used for the Pro Group Algorithm to calculate the relative quantification of the protein expression. The data that support the findings of this study are available in the supplementary material of this article.

2.5 | Bioinformatics analysis of differentially expressed proteins

The Database for Annotation, Visualization, and Integrated Discovery (DAVID; Huang, Sherman, & Lempicki, 2009a, 2009b; RRID:SCR_001881) platform was used to investigate the likely function of proteins that were differentially expressed in each comparison (https://david.ncifcrf.gov/). Gene Ontology (GO) analysis was conducted to include terms that had at least three annotated proteins and a p-value ≤ 0.05. Redundant terms were combined into one term. The Search Tool for the Retrieval of Interacting Genes/Proteins (STRING) 11 (Szklarczyk et al., 2017) (RRID:SCR_005223) was used to identify statistically significant interactions between proteins. Association network analysis was performed with medium confidence (0.400) interaction score to exclude false positive results.

2.6 | Western blotting

Protein extracts were incubated with an equal volume of 2× SDS sample buffer (0.125 M Tris-HCl, 20% glycerol, 4% SDS, 0.004% bromophenol blue, 5% 2-mercaptoethanol in ultrapure water, pH 6.8) for 5 min at 95°C. Samples were centrifugated at 16,000*g* for 1 min at 4°C and loaded onto the 4%–20% Mini-PROTEAN TGX™ Precast polyacrylamide Protein gels (Bio-Rad, #4561096) (14 µg of total protein per lane). Dual Color Standards (Bio-Rad, #1610374) were loaded for molecular weight estimation. Proteins were separated by sodium dodecyl sulfate polyacrylamide gel electrophoresis (SDS-PAGE) in a tank containing running buffer (25 mM Tris, 190 nM glycine, 0.1% SDS in ultrapure water, pH 8.3) at constant voltage (200 V), between 1 and 3 hr depending of the molecular weight of the protein of interest. The separating gel was removed and a piece of gel without the region that contains the protein of interest was cut and stained with Coomassie Brilliant Blue R-250 Staining solution (Bio-Rad, #1610436) as a loading control for the total amount of protein in each lane. Proteins in the other part of the gel were transferred by electrophoresis to the nitrocellulose membrane at constant milliampere (100 mA) overnight at 4°C in a tank containing 192 mM glycine, 25 mM Trizma base in 1 L ultrapure water with addition of 0.5 ml 20% SDS for proteins larger than 80 kDa. Membranes were stained with Ponceau S solution (Sigma, #P7170) to check the quality of the transfer, before blocking with 5% milk powder dissolved in Tris-buffered saline with tween (TBST) at RT for 30 min. Membranes were then incubated with primary antibodies to GFAP or TH (GFAP, Cell signalling (12389), RRID:AB_2631098; GFAP, Biolegend (644701), RRID:AB_2109791; GFAP-delta, Abcam (93251), RRID:AB_11145309; TH, Millipore/Merck (ab152), RRID:AB_390204; Supplementary File S1) in 5% milk/TBST overnight at 4°C with shaking. Membranes were washed three times with TBST (5 min each wash) and incubated with HRP-conjugated secondary antibodies (anti-rabbit, ThermoFisher Scientific (31460), RRID:AB_228341; anti-mouse, ThermoFisher Scientific (31430), RRID:AB_228307; Supplementary File S2) in antibody solution at RT for 1 hr with shaking. Membranes were washed again three times with TBST and incubated with Clarity Western ECL Substrate (Bio-Rad, #1705061) or SuperSignal West Femto (ThermoFisherScientific, #34094) for 5 min. Blots and gels stained with Coomassie were imaged with a CCD system (FluorChem M system, ProteinSimple). Densitometry measurements of antibody reactive bands were obtained using Fiji/ImageJ software (https://imagej.nih.gov/; RRID:SCR_003070) and were normalized to densitometry measurements of the Coomassie stained gel. Uncropped blots and stained gels are provided within the Supplementary file.

2.7 | IHC analysis

Fixed left hemibrains were mounted onto a microtome with Bright Cryo-M-Bed embedding compound (Bright Instrument Company) and sliced in 40 µm coronal sections from a region approximately −4.3 mm to −7.0 mm in relation to bregma (Paxinos & Watson, 2005). Each section was collected consecutively in six wells of a 24-well culture plate containing antifreeze cryoprotectant solution (30% ethylene glycol and 30% glycerol in 0.2 M phosphate buffer) and were subsequently stored at −20°C. For IHC, one of every six sections through the mesencephalic region was processed. This separated sections analyzed by approximately 200 µm to assure that no cell was counted more than once for statistical analyses. Endogenous peroxidase activity was blocked by incubating sections with a solution containing 10% methanol, 10% hydrogen peroxide in TBS for 30 min. After rinsing three times with TBS (5 min each), nonspecific binding sites were blocked in a blocking solution containing 0.2% Triton X-100, 3% normal goat serum in TBS for 20 min. Sections were incubated with an anti-TH primary antibody (Millipore/Merck (ab152), RRID:AB_390204; Supplementary File S1) in blocking solution overnight at 4°C, rinsed three times with TBS (5 min each) and incubated with the biotinylated secondary antibody (Vector Laboratories (PK-6101), RRID:AB_2336820; Supplementary File S2) in TBS for 2 hr at RT. Negative controls were produced by incubating

sections overnight in blocking solution alone, followed by incubation in biotinylated secondary (Supplementary File 3). After three TBS washes of 5 min each, sections were incubated in Vectastain Universal ABC Kit detection system (Vector Labs, #PK6101) for 1 hr at RT. Subsequently, sections were washed three times with TBS (5 min each) and reacted using 3,3-diaminobenzidine tetrahydrochloride (DAB, Sigma, #D8100) as a chromogen. Sections were rinsed three times with TBS to stop the reaction and mounted onto slides. After drying, sections were dehydrated in a series of alcohol gradients (70% for 5 min, 96% for 5 min, 100% for 10 min), immersed in xylene for 10 min, and covered with a coverslip using DPX slide mounting medium (ThermoFisher Scientific). Images were captured using a Nikon Eclipse 80i microscope and Nikon camera connected to a computer with the NiS Elements software. Images were analyzed using Fiji/ImageJ software (https://imagej.nih.gov/). The total number of TH-positive neurons per $(mm)^2$ in each section was tabulated (i.e., all cells were counted in the SNc region of all sections) and the area of soma (expressed in μm^2) of TH-positive neurons determined by drawing around each cell within the dorsal region of the SNc using the "area" tool in NiS Elements software. For both the cell number and soma measurements within one-in-six sections through the nigra region, dopamine neurons were only included in the analysis if they were both TH-positive and it was possible to delimit the soma and proximal processes.

2.8 | Statistical analyses

Statistical analyses were performed using GraphPad Prism version 7.01 (La Jolla, USA) (RRID:SCR_002798). To compare means among the four age groups of animals used, data were analyzed by one-way analysis of variance (ANOVA) test, followed by Tukey's multiple comparisons testing. Differences between groups were statistically significant when the *p*-value was ≤ 0.05.

3 | RESULTS

3.1 | Quantitative proteomics analysis of the rat SNc at four stages of life

To determine whether the rat SNc proteome changes throughout aging, iTRAQ™ quantitative proteomics analysis was used to compare protein expression from four different ages (i.e., postnatal day 14 (juvenile), 8 months old (young adult), 16 months old (middle age), and 21–25 months-old (old)). A total of 2,732 proteins were reliably identified with a 5% local false discovery rate (FDR; see Supplementary Tables S1–S3). For reliable quantification, proteins identified from fewer than three peptides were removed, followed by removal of proteins with fold-change ratios of <1.25 or >0.75, and finally, exclusion of proteins with a *p*-value of <0.05 assigned to their fold changes. This left the following number of proteins that met the criteria for differential expression: 599 proteins in the juvenile compared to young adult group, 31 proteins in the middle age compared to the young adult group, 18 proteins in the old compared to middle age group, and 46 proteins in the old compared to young adult group (Supplementary Tables S4–S7). Review of the 599 proteins differentially expressed in the juvenile compared to the young adult rat SNc group revealed an enrichment of proteins known to be associated with postnatal neurodevelopment (Fuller et al., 2015). Given the overrepresentation of features of normal development in the juvenile versus young adult group, the juvenile data set was excluded from further analyses to retain focus on proteome modifications related to the aging process in adulthood (i.e., middle vs. young adult, old vs. middle age, and old vs. young adult).

Comparison of the middle versus young adult, old versus middle age, and old versus young adult data sets (Supplementary Table S8) found that none of the proteins showed a consistent direction of change across each of the three comparisons, but several proteins were found to be commonly altered across two comparisons (Figures 1 and 2). Proteins with increased expression (Figure 1) include eight that were consistently changed in the old and middle age groups compared to young adults (i.e., apolipoprotein E (APOE), ferritin light chain 1 (FTL1), hyaluronan and proteoglycan link protein 2 (HAPLN2), myelin-associated oligodendrocyte basic protein (MOBP), prosaposin (PSAP), quinoid dihydropteridine reductase (QDPR), ribosomal protein L14 (RPL14) and versican (VCAN) and two that were increased in the old age group compared to middle age and young adult groups (i.e., aspartoacylase (ASPA) and myelin oligodendrocyte glycoprotein (MOG)). Three of the 25 proteins that were increased only in the middle age versus young adult comparison met the criteria for decreased expression in the other two comparisons (i.e., GFAP, huntingtin (HTT) and sodium channel, voltage-gated, type IV, beta subunit (SCN4B); Figure 2); meaning that they increased by middle age but reduced to young adult levels again by old age. One of the seven proteins increased only in the old versus middle age comparison met the criteria for decreased expression in the other two comparisons (i.e., myosin phosphatase rho-interacting protein (MPRIP); Figure 2). Other proteins decreased with age (Figure 2) include two that were consistently changed in old and middle age compared to young (i.e., aldo-keto reductase family 1, member B7 (AKR1B7) and transgelin (TAGLN)) and two proteins that were consistently changed in old compared to middle age and young adult rats (i.e., acetyl-Coenzyme A acyltransferase 2 (ACAA2) and myelin zero protein (MPZ)).

3.2 | Proteins associated with cell adhesion, protein aggregation, and oxidation-reduction are increased in expression with age in the rat SNc

GO analysis using the DAVID highlighted enriched GO biological and molecular processes relating to the proteins increased and decreased with age. These differentially expressed proteins (from Figures 1 and 2) were then subjected to analysis using STRING 11 to identify any known associations between them. Comparison of the resulting

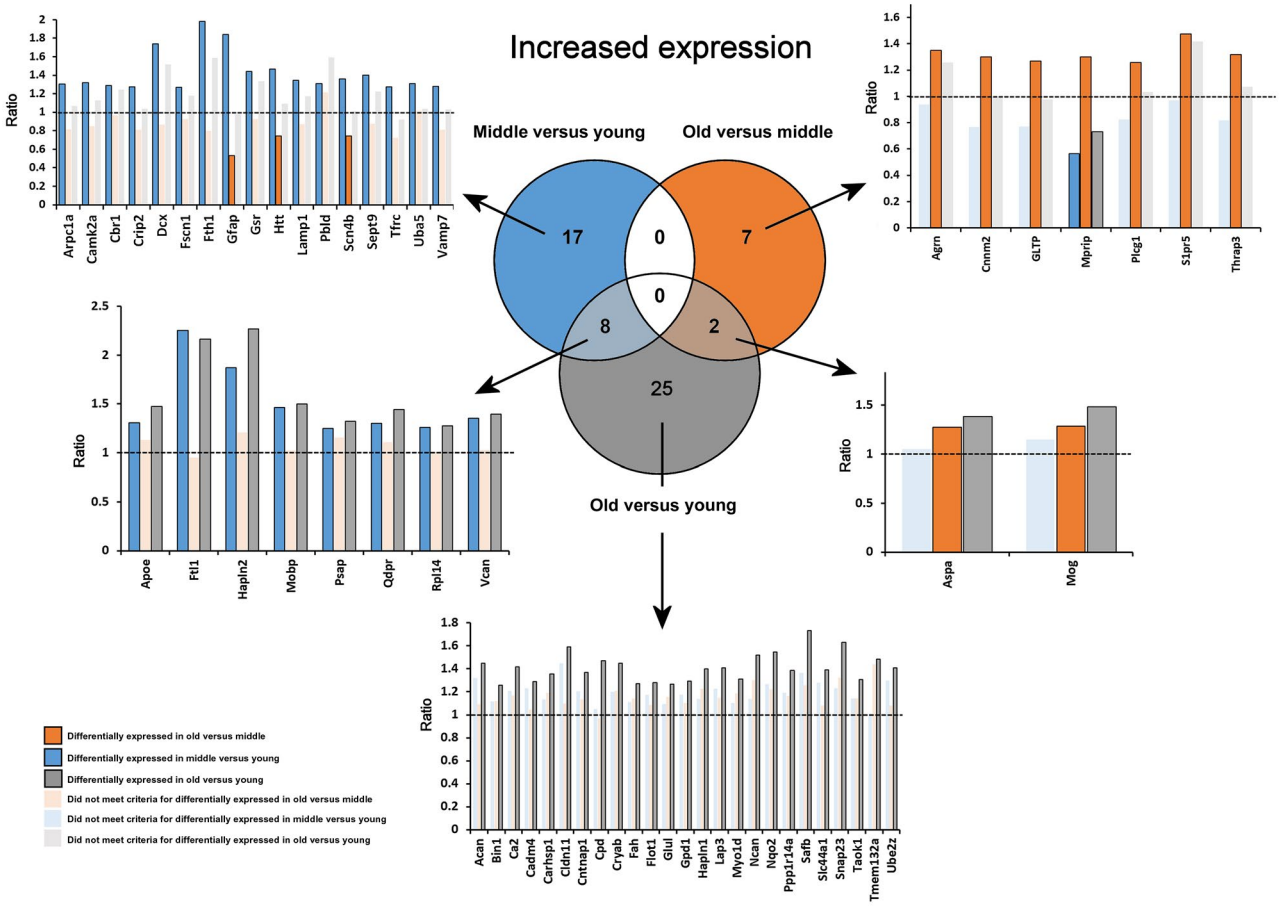

FIGURE 1 Summary of proteins increased in expression in the aging rat substantia nigra (SN). Proteins that met the criteria for increased expression in middle age versus young (blue), old age versus middle (orange), and old age versus young (grey) rat substantia nigra samples are summarized in a Venn diagram and bar charts. The ratios of proteins that met the criteria for increased expression in one comparison but not in others are also shown for reference in the bar charts but are given in light blue, light orange, and light grey, according to the inset legend

networks with the GO analysis output identified protein clusters associated with highly enriched molecular and/or biological processes. For proteins increased in expression (i.e., at one time point compared to a younger time point), enriched processes were associated with cell adhesion/extracellular matrix, and protein aggregation, which included two proteins that specifically mapped to "tau binding" and four that were also associated with oxidation-reduction (Figure 3). Proteins that were decreased in expression at an older compared to a younger time point (Figure 4) were associated with actin binding, metabolism, and astrocyte function (though proteins linked to the latter term, GFAP and vimentin (VIM), were only decreased in the old group compared to middle age group—i.e., they "peaked" at middle age before returning to young adult levels by old age).

3.3 | GFAP is a network hub among proteins differentially expressed with age, and shows differential isoform expression during aging

A key observation from the network analyses of proteins increased in expression at an aged time point was that GFAP was found to have the greatest number of connections to other differentially expressed proteins (Figure 3). In effect, GFAP is shown to be a network hub with experimentally proven links to proteins associated with both protein aggregation (i.e., alpha-crystallin B (CRYAB), HTT, and Ca^{2+}/calmodulin-dependent protein kinase II (CAMK2)) and cell adhesion (i.e., HAPLN2).

We next chose to focus on verifying GFAP expression levels, as GFAP is a marker of astrocytes which are cells that have long been known to provide vital support to neurons (for reviews see; Escartin, Guillemaud, & Carrillo-de Sauvage, 2019; Vernadakis, 1988). Quantitative Western blotting of GFAP in protein extracts from individual SNc samples at different ages revealed a major band in all samples at the predicted molecular weight of 50 kDa (Figure 5a). Densitometry measurements of this band showed a trend of increased expression of GFAP in the middle age adults compared to the young adult and old age groups. Although this peak in expression was not statistically significant, it did match the trend seen in the proteomics data set (Figure 5b). In addition to the major 50 kDa band, three lower molecular weight bands were observed that were more prominent with progressive aging (Figure 5a). Densitometry measurements of all GFAP bands within

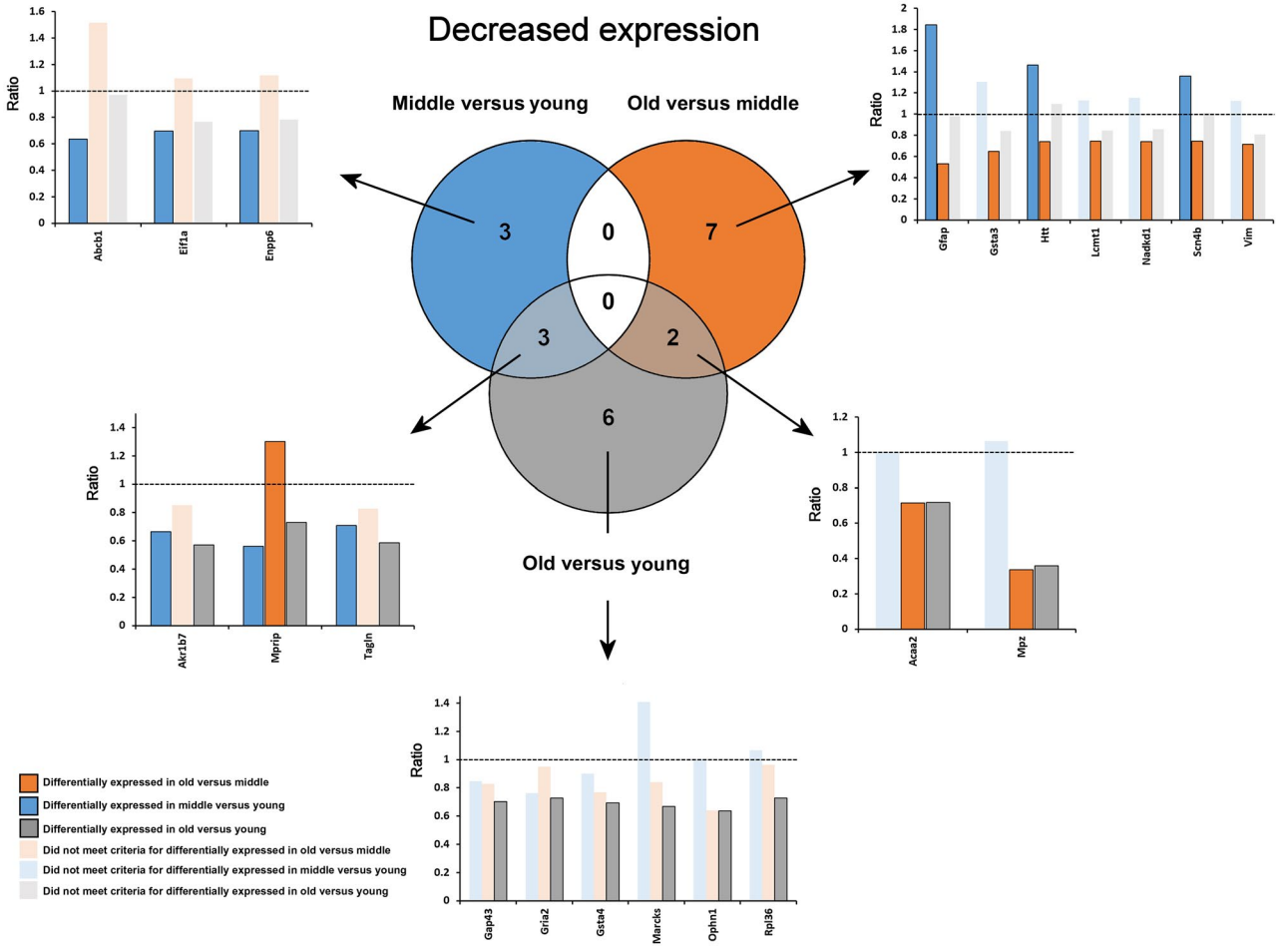

FIGURE 2 Summary of proteins decreased in expression in the aging rat SN. Proteins that met the criteria for decreased expression in middle age versus young (blue), old age versus middle (orange), and old age versus young (grey) rat SN samples are summarized in a Venn diagram and bar charts. The ratios of proteins that met the criteria for decreased expression in one comparison but not in others are also shown for reference in the bar charts but are given in light blue, light orange, and light grey, according to the inset legend

each sample (see example area in red box, Figure 5a) revealed an increase of "total" GFAP expression with increasing age, with the 79% increase between young adult and old samples being statistically significant (p = 0.022; Figure 5c). We are confident that the extra bands are not degradation products resulting from handling and storage conditions because four out of five samples from the old rats were stored for the least amount of time before processing (the fifth being stored for the shortest time out of all ages). In addition, tissue extraction and processing of all samples were undertaken at the same time and under identical conditions. We also ruled out the possibility of an antibody cross-reaction by a different commercially available monoclonal antibody against GFAP, which revealed a very similar distribution of bands (Figure 5d–f). The most plausible explanation for the additional bands, therefore, is that they represent different isoforms of GFAP and/or products of proteolytic cleavage of the canonical, 50 kDa, GFAP protein (Figure 6a). Both scenarios would produce peptides less easily identifiable by mass spectrometry compared to the canonical, 50 kDa protein—i.e., the former would require identification of just one or two unique C-terminal peptides from each isoform (see example sequence alignment in Supplementary File S4), and the latter would reduce the number of trypsin-cleaved peptides of predictable mass for database searching (Figure 6b). This would explain why Western blotting measurements of the 50 kDa band matched the quantitative proteomics result whereas measurement of "total" GFAP did not.

When considering the issue above, it came to our attention that both GFAP-alpha and GFAP-delta (otherwise known as GFAP-epsilon; Hol & Pekny, 2015) isoforms are close in molecular weight (Figure 6a) and would be unlikely to resolve by Western blotting using a "pan" GFAP antibody. We were therefore interested to determine the contribution of each isoform to the increased levels seen in middle age rats. A suitable antibody for detection of rat GFAP-alpha was not available, but analysis of the rat SNc samples with an antibody raised against the GFAP-delta isoform revealed a statistically significant peak of GFAP-delta expression in the SNc of the middle-aged group compared to samples from both young adult (p = 0.0002) and old age samples (p = 0.0008; Figure 5g,h). It

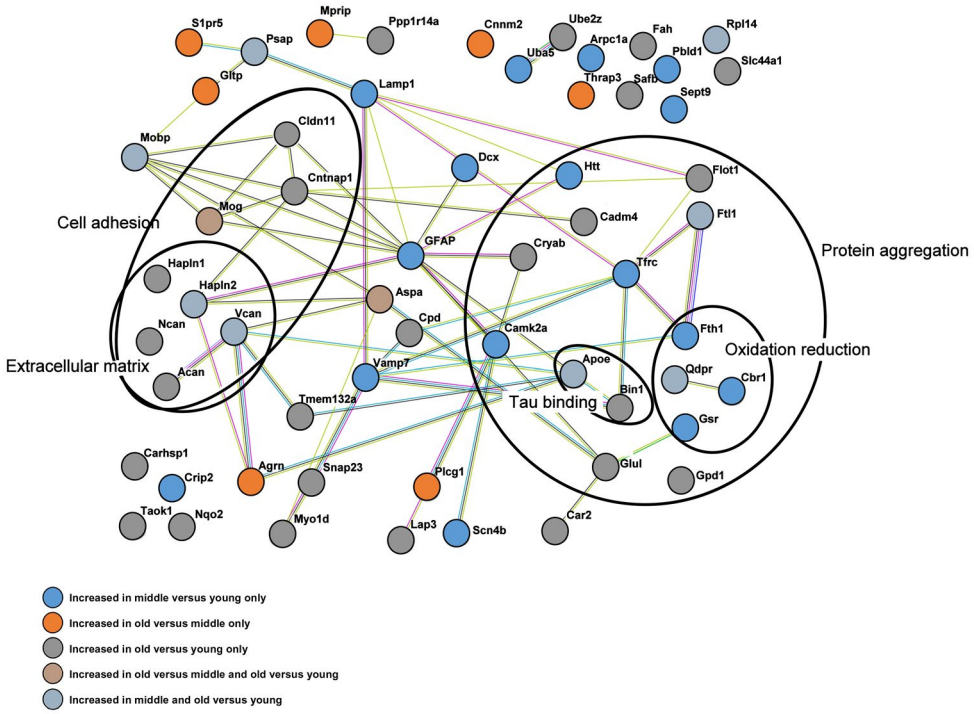

FIGURE 3 Protein network and Gene Ontology (GO) analyses of proteins increased in expression in the rat SN with increasing age. STRING 11 association network showing proteins that met the criteria for increased expression in the middle age versus young (blue); old age versus middle (orange); old age versus young (dark grey); old versus middle and middle versus young (brown); and old and middle versus young (light grey) rat SN with increasing age are shown. The type of association between proteins is indicated by the color (pink: experimentally determined interactors; light blue: interactors form curated database; grey: protein homology; black: co-expression; yellow: text-mining; dark blue: gene co-occurrence; green: gene neighborhood). GO analysis of these proteins using the Database for Annotation, Visualization, and Integrated Discovery (DAVID) revealed an enrichment of terms related to oxidative reduction, cell adhesion, extracellular matrix, tau binding, and protein aggregation (the latter term having been generated following consolidation of the terms identical protein binding and protein homodimerization activity)

is thus possible that when GFAP-alpha and delta are detected together with a "pan" GFAP antibody (as is the case in Figure 5a,d), a stronger signal from GFAP-alpha—which may either be unchanged across ages, or altered to a lesser extent—could partially mask detection of changes to GFAP-delta that are shown here statistically to occur.

3.4 | TH expression levels in the rat SN remain unchanged throughout life

The bioinformatics analysis (above) indicated that proteins associated with cell adhesion and the extracellular matrix were increased in middle and old age compared to the young rat SNc group. We wondered whether this may represent an attempt by cells of the SNc to spread into or fill space, since an age-related decline in dopamine neuron number has been shown to occur in the SNc of a wide range of mammals including rats and primates using strict stereological methods (e.g., Collier et al., 2011; Sanchez et al., 2008; Figure 7). It was interesting to observe a potential contradiction from the proteomics data; however, in that the expression levels of TH—a marker of dopamine neurons—in the rat SNc remained unchanged throughout aging (Supplementary Tables S1–S3). This finding was verified by quantitative Western blotting (Figure 7a,b). We also quantified and compared the number and size of TH-positive neurons from the dorsal region of the SNc using IHC. In agreement with previous stereological studies (Collier et al., 2011; Sanchez et al., 2008), this showed a significant decrease in the number of dopamine neurons between the young adult (0.0004 ± 0.0002) stage and middle age (0.0003 ± 0.0001; $p < 0.0001$; Figure 7c,d). Measurements of the soma size of TH-positive neurons in the SNc, however, found that reduced dopamine neuron number was accompanied by a significant increase in the area of the soma of TH-positive neurons in both old (201 ± 50.53) and middle-aged (198.3 ± 51.85) rats compared to the young adult group (164 ± 35.89, $p < 0.0001$; Figure 7e,f). When combined, these histological and proteomic findings suggest that dopamine neurons reduce in number, but that surviving neurons increase in size and maintain TH expression (i.e., suggesting more dopamine production per neuron) during the aging process.

4 | DISCUSSION

Idiopathic PD is correlated with advancing age, and so here we have sought to determine whether changes occur within the proteome of the SNc region during normal aging to provide some clues into this

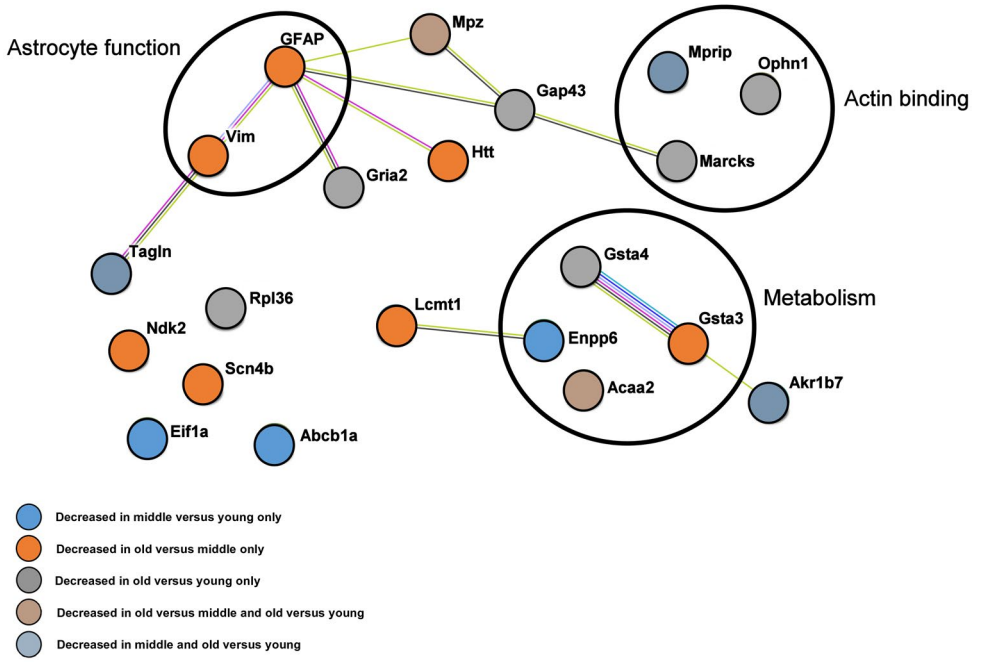

FIGURE 4 Protein network and Gene Ontology (GO) analyses of proteins decreased in expression in the rat SN with increasing age. STRING 11 association network showing proteins that met the criteria for decreased expression in the middle age versus young (blue); old age versus middle (orange); old age versus young (dark grey); old versus middle and middle versus young (brown); and old and middle versus young (light grey) rat SN with increasing age are shown. The type of association between proteins is indicated by the color (pink: experimentally determined interactors; light blue: interactors form curated database; grey: protein homology; black: co-expression; yellow: text-mining; dark blue: gene co-occurrence; green: gene neighborhood). GO analysis of these proteins using the Database for Annotation, Visualization, and Integrated Discovery (DAVID) revealed an enrichment of terms related to astrocyte function, metabolism, and actin binding

association. Collectively, proteomics and bioinformatics, combined with Western blotting and histological analyses, identified significant proteome changes in the SNc of rats by 16 months of age. Such alterations at this age appear to be relatively "young" in terms of human years, as studies establishing relative age between animals indicate that 16 months in rats are equivalent to ~40 years in humans (Sengupta, 2013). When categorizing the protein changes that occur during aging, there appears to be an increase in proteins associated with oxidation-reduction processes, protein aggregation, and cell adhesion/extracellular matrix (Figures 1 and 3). These changes occur concomitantly with reduced expression of proteins involved in astrocyte function, actin binding, and metabolism (Figures 2 and 4). Analysis of the intermediate filament protein, GFAP, revealed that it is a network hub for proteins differentially expressed throughout aging, and that GFAP isoform expression is altered during normal aging. Interestingly, while there was a reduction in the number of dopamine neurons as aging progressed, the remaining dopamine neurons were significantly increased in size and the level of TH expression in the SNc region was maintained throughout all adult ages. When considered together, these findings suggest the potential for an insidious process of protein changes (starting by middle age) in the SNc that, over time, ultimately results in a protein profile among cells in the SNc that would challenge the viability of dopamine neurons.

4.1 | Proteins associated with oxidation-reduction processes, protein aggregation, and tau binding increase in expression during aging

Bioinformatics analysis revealed that proteins associated with reducing oxidative stress are increased in expression at middle age (i.e., glutathione reductase (GSR) and carbonyl reductase 1—Cbr1), and in both middle and old ages (QDPR) compared to young adults (Figures 1 and 3). Interestingly, increased expression of these reductases, known to combat oxidative stress (Couto, Wood, & Barber, 2016; Rashid, Haque, & Akbar, 2016; Si, Sun, & Gu, 2017; Xu et al., 2014), occur in conjunction with increased expression of ferritin heavy chain 1 (FTH1), a subunit of ferritin whose accumulation results in poor iron sequestration in cells and cell death (Lewerenz, Ates, Methner, & Conrad, 2018). These changes may be particularly important in relation to the viability of SNc neurons as oxidative stressors and iron accumulation are both known to play a major role in age-related neuronal death (Liguori et al., 2018; Salminen & Paul, 2014) and PD (Liu, Liang, & Soong, 2019; Sun et al., 2019; Wojtunik-Kulesza, Oniszczuk, & Waksmundzka-Hajnos, 2019; for review see Reeve, Simcox, & Turnbull, 2014). The glutathione system is known to be key in protecting cells from ferroptosis (a non-apoptosis form of cell destruction; Cardoso, Hare, Bush, & Roberts, 2017). This is directly relevant to midbrain dopamine neurons where it has been

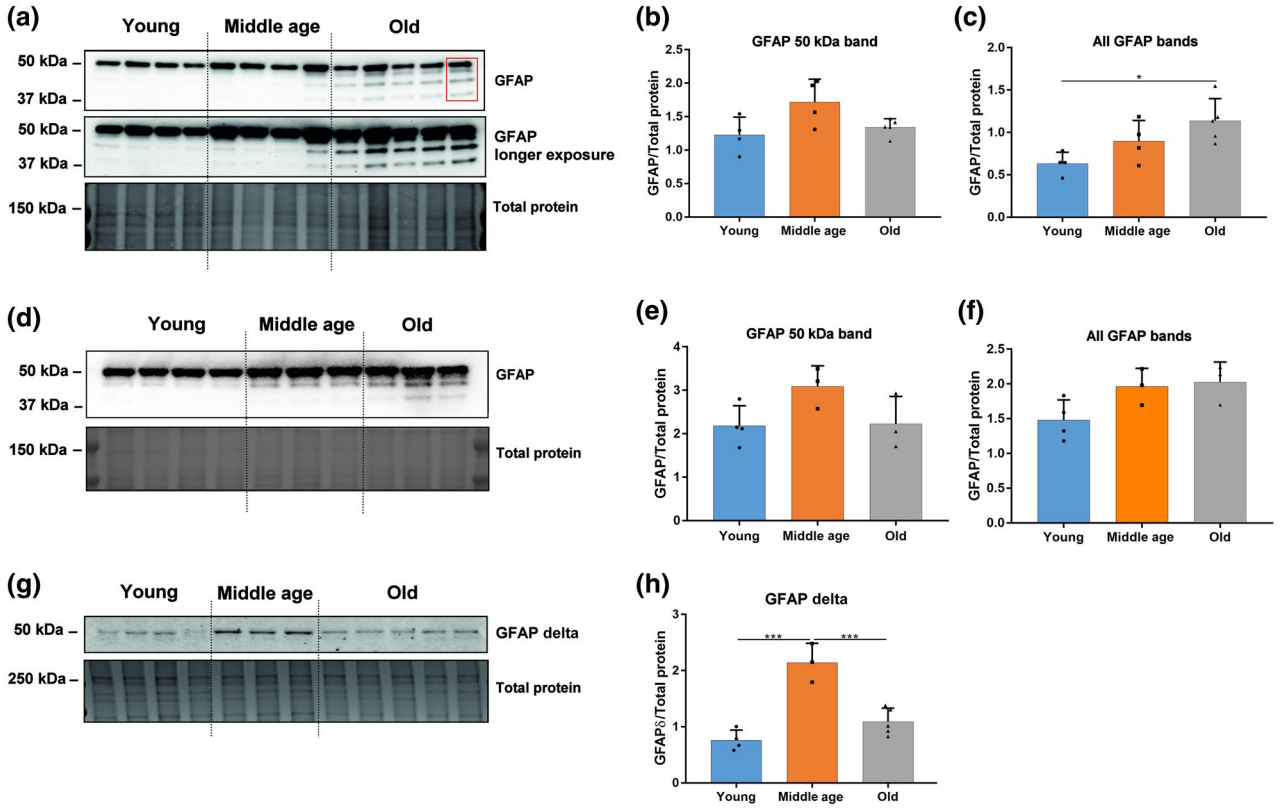

FIGURE 5 Western blotting of glial fibrillary acidic protein (GFAP) expression in the substantia nigra (SNc) of young adult, middle age, and old rats. (a) Representative Western blot showing the expression levels of GFAP in the SNc of young adult (n = 4), middle age (n = 4), and old rats (n = 5), detected with a rabbit monoclonal antibody from Cell Signalling Technology (#12389). A main band was detected in all samples at 50 kDa, with additional lower molecular weight bands present that were more intense in the samples from old rats. (b) The integrated density of measured GFAP 50 kDa band from (a), normalized to total protein (Coomassie stained gel), showed a non-statistically significant increase in the middle age samples compared to young adult (p = 0.0571) and old (p = 0.1398). (c) The integrated density of all measured GFAP bands from (a) (see example in red box for area of measurement), normalized to total protein (Coomassie stained gel), showed a statistically significant increase between the young adult and old samples (p = 0.0221). (d) Representative Western blot showing the expression levels of GFAP in the SN pars compact (SNc) of young adult (n = 4), middle age (n = 3), and old rats (n = 3), detected with a mouse monoclonal antibody from Biolegend (#644701). Similarly, to panel (a), A main band was detected in all samples at 50 kDa, with additional lower molecular weight bands present that were more intense in the samples from old rats. (e) The integrated density of measured GFAP 50 kDa band from (d), normalized to total protein (Coomassie stained gel), showed a non-statistically significant increase in the middle age samples compared to young adult (p = 0.1562) and old (p = 0.2218). (f) The integrated density of all measured GFAP bands from (D), normalized to total protein (Coomassie stained gel), showed a non-statistically significant increase between the young adult and old samples (p = 0.1119). (g) Representative Western blot showing the expression levels of GFAP-delta in the SN of young adult (n = 4), middle age (n = 3), and old rats (n = 5), detected with a rabbit polyclonal antibody from Abcam (#93251). (h) The integrated density of measured GFAP-delta from (g), normalized to total protein (Coomassie stained gel), showed a statistically significant increase in the middle age samples compared to young adult (182%; p = 0.0002) and a statistically significant decline from middle age to old samples (49%; p = 0.0008). Error bars represent standard deviation. *p < 0.05; ***p < 0.001

shown that a depletion of glutathione activity enhances oxidative stress (via arachidonic acid) and promotes dopamine neuron death (Mytilineou, Kramer, & Yabut, 2002). In the future, therefore, it will be important to monitor changes in oxidative stress regulators and iron accumulation during normal human aging to explore the potential to modulate these cellular systems and nullify any age-related contribution to increased neuronal vulnerability.

It was also interesting to note that proteins associated with protein aggregation and, in particular, tau binding (i.e., apolipoprotein E (APOE) and bridging integrator 1 (BIN1)) are also increased in expression during normal aging of the SNc. The importance of protein aggregation to neural degeneration is well illustrated in the experiments by Roostaee, Beaudoin, Staskevicius, and Roucou (2013) which show that alpha-synuclein dimerization initiates the formation of aggregates and fibrils in neurons *in vitro*, and that neurotoxicity results in the brain of mice where this process is facilitated. While the processes of protein aggregation (in particular tau binding) have long been associated with AD (Gonzalez, Abud, Abud, Poon, & Gyly, 2017), findings are beginning to emerge showing that tau pathology is also associated with PD (for review see; Zhang et al., 2018). Recent work has shown that APOE, in particular, is elevated in patients with untreated (early) PD, and that the lipoprotein may provide a mechanism by which alpha-synuclein can be taken up into SN dopamine neurons

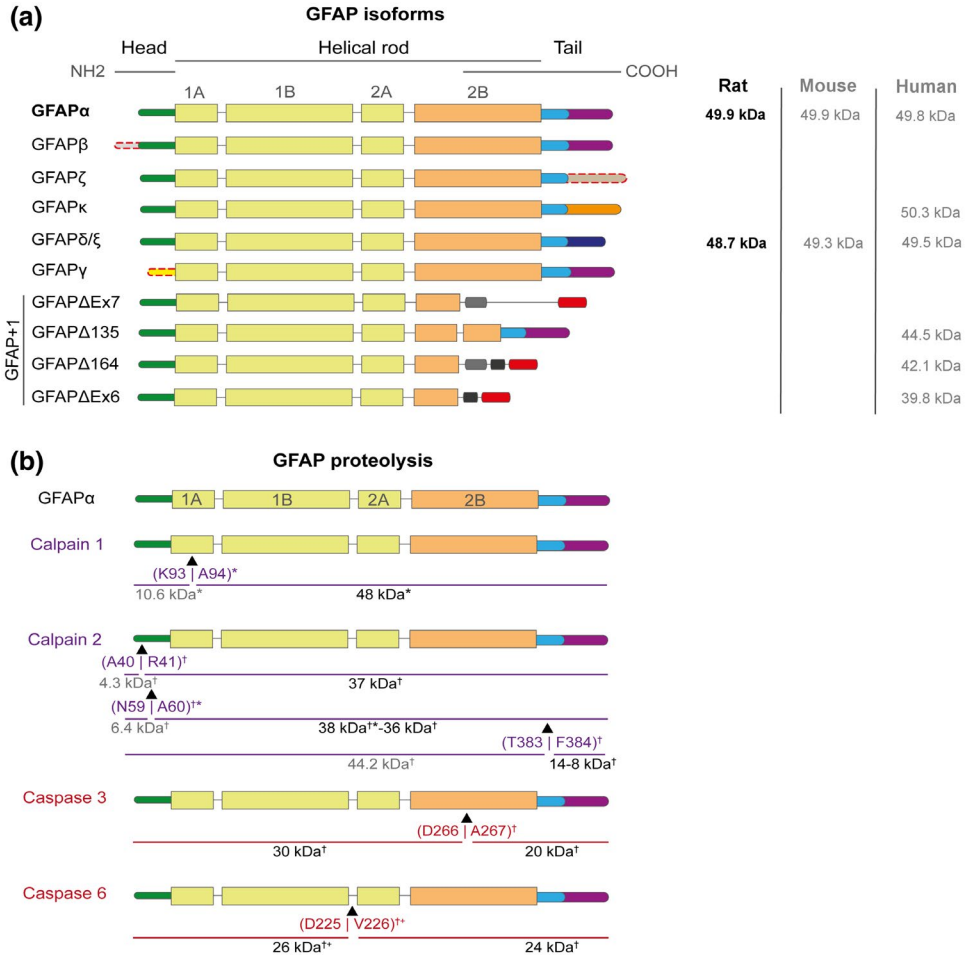

FIGURE 6 Schematic diagrams summarizing glial fibrillary acidic protein (GFAP) variants and degradation products: (a) The GFAP protein has a head, rod, and tail domain, and the various GFAP isoforms differ according to their sequence and sequence length at the N- and/or C-terminal regions. The head domain (green) contains the exon 1; the rod domain is divided in four sub-regions (1A (exon 2), 1B (exon 3), 2A (exon 4), 2B (exons 5 and 6)), separated by linker regions (black lines); and the tail domain contains exons 7 to 9. Only GFAP-alpha (α) (bold font) and GFAP-delta (δ) have known molecular weights in the rat (i.e., 49.9 kDa (Uniprot P47819-1) and 48.7 kDa (Uniprot KB–P47819-2), respectively). NB. GFAPδ and ε have previously been referred to as the same isoform (Hol & Pekny, 2015), but a polyadenylation in exon 7a may mean that GFAPε should be considered as a separate isoform (Blechingberg, Lykke-Andersen, Jensen, Jørgensen, & Nielsen, 2007). Where readily available in publications or protein databases, molecular weights of GFAP isoforms reported in mouse and human are shown in grey font (Hol & Pekny, 2015; Hol et al., 2003; Kamphuis et al., 2012, 2014). Evidence for the existence of isoforms shown without a corresponding molecular weight come from partial transcripts (summarized by Hol & Pekny, 2015). (b) Possible calpain and caspase proteolytic degradation products of GFAP are shown, along with their known (black) or predicted (grey) molecular weight. Known molecular weights were obtained from Lee et al. (2000) (calpain 1), Fujita et al. (1998) and Zhang et al. (2014) (calpain 2), Mouser, Head, Ha, and Rohn (2006) (caspase 3) and Chen, Hagemann, Quinlan, Messing, and Perng (2013) (caspase 6). Molecular weight predictions (for fragments not reported in the literature) were made using a protein molecular weight calculator (https://www.bioinformatics.org/sms/prot_mw.html) without considering post-translational modifications. The molecular weight of GFAP fragments may vary according to the species, are here are indicated as follows: rat (*), mouse (+), or human (†) origin

(Paslawski et al., 2019). Similarly, though high expression levels of BIN1 has proven to be a good indicator of increased susceptibility to AD (Chapuis et al., 2013), studies examining the association of BIN1 and genetic contributors to PD (i.e., the glucocerebrosidase (GBA); Sidransky & Lopez, 2012) have shown that the age of onset of GBA-associated PD can be altered by BIN1 expression (Gan-Or et al., 2015). When combined, these studies suggest that there is some overlap in the proteins associated with AD and PD, and, in combination with the findings here, that there is growing evidence for a close association between abnormal protein expression in neurodegenerative disease and normal aging of the brain.

Understanding the interplay between oxidative processes and protein aggregation could also be useful for understanding and combating age-neuronal loss and neurodegenerative disease. Work by Rajagopal, Deb, Poddar, and Paul (2016), for example, looking at changes in protein dimerization in the cortex and hippocampus (areas affected by AD) of normal rats up to 18 months old, showed that there is increased dimerization/aggregation of

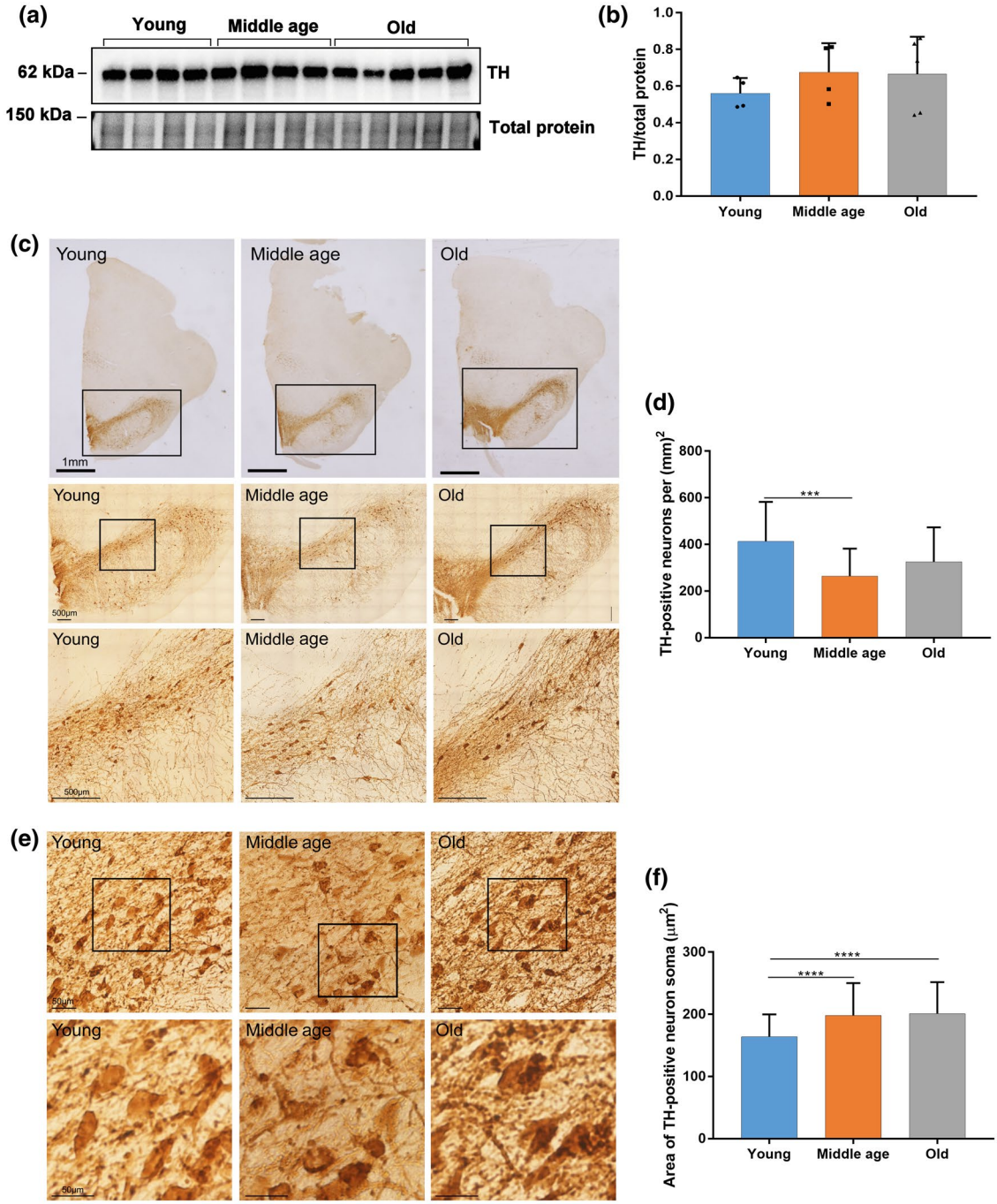

FIGURE 7 Levels of tyrosine hydroxylase (TH) expression remain stable throughout aging, while the number of TH + neurons are reduced but increase in soma size: (a) Representative Western blot showing the expression levels of TH in the substantia nigra pars compact (SNc) of young adult (n = 4), middle age (n = 4), and old rats (n = 5), detected with a rabbit polyclonal antibody from Millipore/Merck (ab152). (b) The integrated density of the TH bands from (a), normalized to total protein (Coomassie stained gel), showed no significant difference in TH expression levels across each age group. (c and e) Representative anti-TH stained coronal sections taken from the SN at the rostral-caudal level where the optic tract enters the midbrain. Boxes in images indicate area shown in high magnification in subsequent rows. (d and f) Statistical comparison of the average number of TH+ neurons per $(mm)^2$ and the average area of TH+ cell soma (μm^2) in the dorsal SNc (boxed area in middle row of c) of young adult, middle age, and old age rats. Size of scale bar shown in first image of each row. ***$p < 0.01$, ****$p < 0.001$

the phosphatase striatal-enriched tyrosine phosphatase (STEP—a phosphatase that protects neurons from excitotoxicity) during aging. This increased dimerization of STEP, causing a loss of its function, results in a depletion of glutathione and an increase in oxidative stress in the brain. When the glutathione system was enhanced through the application of *N*-acetyl cysteine, this was found to reduce the dimerization of STEP and stop negative downstream effects.

4.2 | The intermediate filament protein GFAP changes throughout aging

Here we have identified that GFAP links the greatest number of proteins altered during aging (Figure 3). Previous studies have indicated that there is an increase in the expression of GFAP in the human SNc at old age (Jyothi et al., 2015). This matches the findings from the Western blotting here showing that the expression levels of GFAP gradually increase throughout the three adult stages analyzed (Figure 5). Examination of the GFAP-delta isoform specifically, however, found that there was a significant increase in its expression during middle age (in comparison to young adult and old-aged rats; Figure 5). This is important to note, as it highlights that changes can occur in astrocytes earlier than previously thought, and that changes in protein isoforms can be masked if analysis is conducted using "pan" GFAP antibodies alone.

Although the alpha isoform of GFAP is considered the canonical form of the protein, delta does occur in the brain but is typically expressed at significantly lower levels than alpha (<10%; Perng et al., 2008), and is associated with disease states (e.g., astrocytomas; Choi, Kwak, Kim, Sheen, & Kang, 2009). When expression of the delta isoform is increased above 10% of total GFAP it can disrupt the assembly of intermediate filaments within astrocytes (particularly the assembly of GFAP-alpha) and elicits an increase in alpha-crystallin B sedimentation (Perng et al., 2008). This sequence of events aligns well with the iTRAQ^{TM} results here showing that CRYAB also increases during aging along with GFAP-delta. This process is important to highlight because CRYAB sedimentation is known to cause protein aggregations that disrupt normal cell function, and its upregulated a feature of the post-mortem Parkinson's SNc (Liu et al., 2015). If sedimentation occurs in astrocytes during normal aging, it could negatively alter the supportive functions of astrocytes that are fundamental to dopamine neuron viability (Mena, Bernardo, Casarejos, Canals, & Rodríguez-Martín, 2002). This may be particularly important in relation to oxidative stress (highlighted above), where it is well established that neurons are highly dependent on astrocytes for protection from oxidative stress, and (in some cases) may be the only source of antioxidation via glutathione transferase activity (Murphy et al., 2001). Interestingly, while postmortem analyses of regions of the parkinsonian brain relatively spared from neurodegeneration (i.e., the caudate, putamen, and frontal cortex) show an increase in astrocyte activity and glutathione levels (Mythri et al., 2011), the proteomics analyses conducted here show a decrease in both glutathione transferase 3 and 4 during normal aging (Figures 1–4).

The role that astrocytes and the changing isoform of GFAP plays in the aging process, however, is complicated by the fact that there also appears to be a close relationship between protein homodimerization (abnormal protein aggregation) and GFAP-delta. Perng et al. (2008) noted that the delta tail of GFAP may in fact inhibit homodimerization. This would make sense in light of the findings here showing that increases in protein aggregation occur at middle age, which overlaps with a period of significantly increased expression of the GFAP-delta isoform. This finding suggests the possibility that increases in the expression of the GFAP-delta may occur as a positive response to increased protein aggregation, adding to the list of protective responses by astrocytes in the brain. Whether astrocytes are becoming more dysfunctional through the increased expression of the GFAP-delta isoform or are attempting to combat increases in protein aggregation in the SNc during aging is still unclear. In the future, it will be important to fully characterize the changes in astrocytes during aging and determine at what stage they occur. This could not only be useful for identifying markers of a "pre-parkinsonian" state (Collier et al., 2011), but may also help identify contributors to age-related neuronal loss or endogenous responses meant to combat it.

4.3 | Dopamine neurons maintain TH expression levels in the SNc region during aging, even though neuronal numbers are significantly reduced and proteins associated with metabolism are decreased in expression

iTRAQ^{TM} and quantitative Western blotting of the rate-limiting enzyme for dopamine production, TH, showed that it was not altered in expression during the aging process (Figure 7). This was somewhat surprising as it has long been established that there is a "normal" age-related decline in dopamine neuron numbers in rats and humans (Collier et al., 2017; Sanchez et al., 2008). Due to this, and because the by-products of dopamine production can have an impact on the oxidative stress levels of dopamine neurons (for review; see Dias, Junn, & Mouradian, 2013), we sought to further characterize dopamine neurons in tissue sections taken from the same animals used for proteomics and Western blotting (Figure 7). When counting the number of TH-positive cell bodies in the core of the SNc in young adult, middle age, and old rats, we indeed found a decrease in the number of dopamine neurons between young adult versus middle age (Figure 7). Interestingly, however, when the size of these neuronal cell bodies was also measured, we found that there was a significant increase in the soma at progressive ages (Figure 7) similar to that seen in humans (Cabello, Thune, Pakkenberg, & Pakkenberg, 2002). When combined, these findings suggest that there is an increased level of the dopamine synthesis pathway by fewer dopamine neurons in the SNc, presumably to maintain an appropriate "pool" of dopamine for basal ganglia functioning (Zhai, Tanimura, Graves, Shen, & Surmeier, 2018). This possibility is supported by the fact that we have shown an age-related increase in QDPR, which is a known catalyst for tetrahydrobiopterin recycling and subsequent TH synthesis (Breuer et al., 2019; Ishikawa et al., 2016). Any increase in dopamine synthesis would likely place a high demand on neuronal cells and astrocyte function to both produce neurotransmitter and control the stressors related to that production. This was somewhat confounding in the present analyses as proteins associated with cellular metabolism appear to be reduced in expression in

the SNc during aging (Figure 4). Whether metabolic reduction is due to cellular dysfunction or simply due to cell loss in the region is unclear, but such alterations conflict with the increases in protein expression in the region. Added to this is the finding that proteins associated with the extracellular matrix are also increased in expression during aging. This trend is in line with our past research showing changes in the expression proteins related to the extracellular matrix in the striatum of rats after inducing dopamine neuron degeneration (Fuller et al., 2014). Such responses in the adult brain could represent an attempt to reorganize circuitry or cell connectivity, which has been shown to occur at the level of the dendritic spine during normal rodent aging (Davidson, Mejía-Gómez, Jacobowitz, & Mostany, 2019).

4.4 | Aging presents a growing challenge to cell viability and function in the SNc

When taken together, the results of our study indicate that there are changes to the proteome of the normally aging rat SNc that would increasingly challenge the viability of cells in the region. Proteins related to oxidative stress, protein aggregation, and astrocytic function all become altered during aging; each of which are processes likely to negatively impact dopamine neuron survival. In particular, changes in the expression of proteins related to oxidative processes occur alongside alteration in the level of expression of GFAP and its isoforms. This would present further challenges to cell viability in the region as astrocytes are important to the homeostatic environment, particularly in relation to oxidative stress. This may be particularly important to consider in human aging and PD due to the fact that many human SNc dopamine neurons convert dopamine into a more stable form, neuromelanin. This reduction of dopamine to neuromelanin produces highly oxidative by-products and would add to the oxidative stresses brought on by normal aging. This additive effect (brought on by normal aging and dopamine reduction) might explain why rats (and other mammals that do not produce neuromelanin) do not naturally show signs of sporadic PD during aging, and why there is a selective degeneration of neuromelanin containing neurons in PD (Hirsch, Graybiel, & Agid, 1988; Hirsch, Graybiel, & Agid, 1989; for reviews see Vila, 2019; Monzani et al., 2019). Interestingly, the loss of neurons during normal aging (Cabell et al., 2002; and Figure 7) would increase the demand for more dopamine synthesis per remaining neuron (as suggested here), resulting in a cycle of increased oxidative stressors in the human SNc and further neuronal loss. If such an age-related cycle were accelerated (as suggested by Collier et al., 2011, 2017), it could produce more rapid destruction of dopamine neurons in the human SNc (Segura-Aguilar et al., 2014; Zhang, Wang, & Wang, 2019) and result in a parkinsonian state.

DECLARATION OF TRANSPARENCY

The authors, reviewers and editors affirm that in accordance to the policies set by the Journal of Neuroscience Research, this manuscript presents an accurate and transparent account of the study being reported and that all critical details describing the methods and results are present.

ACKNOWLEDGMENTS

This work was made possible by generous funding from the Keele University ACORN scheme and Keele University School of Medicine.

CONFLICT OF INTEREST

The authors have no conflict of interest to declare for this manuscript.

AUTHOR CONTRIBUTIONS

Conceptualization, M.A.G; *Validation*, M.A.G, Y.G.G, H.R.F.; *Investigation*, M.A.G, Y.G.G, and H.R.F.; *Formal Analysis*, M.A.G, Y.G.G, H.R.F., S.S., S.L.S; *Resources*, H.R.F. and M.A.G.; *Writing—Original Draft Preparation*, M.A.G, Y.G.G, and H.R.F; *Writing—Review & Editing*, M.A.G, Y.G.G, H.R.F, S.S., S.L.S; *Visualization*, M.A.G, Y.G.G, and H.R.F; *Supervision*, H.R.F. and M.A.G; *Project Administration*, M.A.G.; *Funding Acquisition*, M.A.G.

DATA AVAILABILITY STATEMENT

The mass spectrometry proteomics data have been deposited to the ProteomeXchange Consortium via the PRIDE (Perez-Riverol et al., 2019) partner repository with the data set identifier PXD017018.

ORCID

Heidi R. Fuller https://orcid.org/0000-0002-2858-869X
Monte A. Gates https://orcid.org/0000-0002-2901-1083

REFERENCES

Beach, T. G., Walker, D. G., Sue, L. I., Newell, A., Adler, C. C., & Joyce, J. N. (2004). Substantia nigra Marinesco bodies are associated with decreased striatal expression of dopaminergic markers. *Journal of Neuropathology and Experimental Neurology*, *63*, 329–337.

Blechingberg, J., Lykke-Andersen, S., Jensen, T. H., Jørgensen, A. L., & Nielsen, A. L. (2007). Regulatory mechanisms for 3′-end alternative splicing and polyadenylation of the glial fibrillary acidic protein, GFAP, transcript. *Nucleic Acids Research*, *35*, 7636–7650.

Bradford, M. M. (1976). A rapid and sensitive method for the quantitation of microgram quantities of protein utilizing the principle of protein-dye binding. *Analytical Biochemistry*, *72*, 248–254.

Breuer, M., Guglielmi, L., Zielonka, M., Hemberger, V., Kölker, S., Okun, J. G., … Opladen, T. (2019). QDPR homologues in Danio rerio regulate melanin synthesis, early gliogenesis, and glutamine homeostasis. *PLoS ONE*, *14*, e0215162. https://doi.org/10.1371/journal.pone.0215162

Cabello, C. R., Thune, J. J., Pakkenberg, H., & Pakkenberg, B. (2002). Ageing of substantia nigra in humans: Cell loss may be compensated by hypertrophy. *Neuropathology and Applied Neurobiology*, *28*, 283–291.

Cardoso, B. R., Hare, D. J., Bush, A. I., & Roberts, B. R. (2017). Glutathione peroxidase 4: A new player in neurodegeneration? *Molecular Psychiatry*, *22*, 328–335.

Chapuis, J., Hansmannel, F., Gistelinck, M., Mounier, A., Van Cauwenberghe, C., Kolen, K. V., …GERAD Consortium. (2013). Increased expression of BIN1 mediates Alzheimer genetic risk by modulating tau pathology. *Molecular Psychiatry*, *18*, 1225–1234.

Chen, M. H., Hagemann, T. L., Quinlan, R. A., Messing, A., & Perng, M. D. (2013). Caspase cleavage of GFAP produces an assembly-compromised proteolytic fragment that promotes filament aggregation. *ASN Neuro*, *5*, e00125. https://doi.org/10.1042/AN20130032

Choi, K. C., Kwak, S. E., Kim, J. E., Sheen, S. H., & Kang, T. C. (2009). Enhanced glial fibrillary acidic protein-delta expression in human astrocytic tumor. *Neuroscience Letters*, *463*, 182–187.

Chu, Y., & Kordower, J. H. (2007). Age-associated increases of alpha-synuclein in monkeys and humans are associated with nigrostriatal dopamine depletion: Is this the target for Parkinson's disease? *Neurobiology of Disease*, *25*, 134–149.

Collier, T. J., Kanaan, N. M., & Kordower, J. H. (2011). Ageing as a primary risk factor for Parkinson's disease: Evidence from studies of non-human primates. *Nature Reviews Neuroscience*, *12*, 359–366.

Collier, T. J., Kanaan, N. M., & Kordower, J. H. (2017). Aging and Parkinson's disease: Different sides of the same coin? *Movement Disorders*, *32*, 983–990.

Couto, N., Wood, J., & Barber, J. (2016). The role of glutathione reductase and related enzymes on cellular redox homoeostasis network. *Free Radical Biology and Medicine*, *95*, 27–42.

Davidson, A. M., Mejía-Gómez, H., Jacobowitz, M., & Mostany, R. (2019). Dendritic spine density and dynamics of layer 5 pyramidal neurons of the primary motor cortex are elevated with aging. *Cerebral Cortex*. https://doi.org/10.1093/cercor/bhz124. [Epub ahead of print].

Dias, V., Junn, E., & Mouradian, M. M. (2013). The role of oxidative stress in Parkinson's disease. *Journal of Parkinson's Disease*, *3*, 461–491.

Escartin, C., Guillemaud, O., & Carrillo-de Sauvage, M. A. (2019). Questions and (some) answers on reactive astrocytes. *Glia*, *67*, 2221–2247.

Fujita, K., Yamauchi, M., Matsui, T., Titani, K., Takahashi, H., Kato, T., … Nagata, Y. (1998). Increase of glial fibrillary acidic protein fragments in the spinal cord of motor neuron degeneration mutant mouse. *Brain Research*, *785*, 31–40.

Fuller, H. R., Hurtado, M. L., Wishart, T. M., & Gates, M. A. (2014). The rat striatum responds to nigro-striatal degeneration via the increased expression of proteins associated with growth and regeneration of neuronal circuitry. *Proteome Science*, *12*, 20.

Fuller, H. R., Slade, R., Jovanov-Milošević, N., Babić, M., Sedmak, G., Šimić, G., … Gates, M. A. (2015). Stathmin is enriched in the developing corticospinal tract. *Molecular and Cellular Neuroscience*, *69*, 12–21.

Gan-Or, Z., Amshalom, A., Bar-Shira, M., Gana-Weisz, A., Mirelman, K., Marder, S., … Orr-Urtreger, A. (2015). The Alzheimer disease BIN1 locus as a modifier of GBA-associated Parkinson disease. *Journal of Neurology*, *262*, 2443–2447.

Gonzalez, B., Abud, E. M., Abud, A. M., Poon, W. W., & Gyly, K. H. (2017). Tau spread, apolipoprotein E, inflammation, and more: Rapidly evolving basic science in Alzheimer disease. *Neurologic Clinics*, *35*, 175–190.

Hindle, J. V. (2010). Ageing, neurodegeneration and Parkinson's disease. *Age and Ageing*, *39*, 156–161.

Hirsch, E., Graybiel, A. M., & Agid, Y. A. (1988). Melanized dopaminergic neurons are differentially susceptible to degeneration in Parkinson's disease. *Nature*, *334*, 345–348.

Hirsch, E. C., Graybiel, A. M., & Agid, Y. (1989). Selective vulnerability of pigmented dopaminergic neurons in Parkinson's disease. *Acta Neurologica Scandinavia*, *126*, 19–22.

Hol, E. M., & Pekny, M. (2015). Glial fibrillary acidic protein (GFAP) and the astrocyte intermediate filament system in diseases of the central nervous system. *Current Opinion in Cell Biology*, *32*, 121–130.

Hol, E. M., Roelofs, R. F., Moraal, E., Sonnemans, M. A., Sluijs, J. A., Proper, E. A., … van Leeuwen, F. W. (2003). Neuronal expression of GFAP in patients with Alzheimer pathology and identification of novel GFAP splice forms. *Molecular Psychiatry*, *8*, 786–796.

Huang, D. W., Sherman, B. T., & Lempicki, R. A. (2009a). Systematic and integrative analysis of large gene lists using DAVID bioinformatics resources. *Nature Protocols*, *4*, 44–57.

Huang, D. W., Sherman, B. T., & Lempicki, R. A. (2009b). Bioinformatics enrichment tools: Paths toward the comprehensive functional analysis of large gene lists. *Nucleic Acids Research*, *37*, 1–13.

Ishikawa, T., Imamura, K., Kondo, T., Koshiba, Y., Hara, S., Ichinose, H., … Inoue, H. (2016). Genetic and pharmacological correction of aberrant dopamine synthesis using patient iPSCs with BH4 metabolism disorders. *Human Molecular Genetics*, *25*, 5188–5197.

Jyothi, H. J., Vidyadhara, D. J., Mahadevan, A., Philip, M., Parmar, S. K., Manohari, S. G., … Alladi, P. A. (2015). Aging causes morphological alterations in astrocytes and microglia in human substantia nigra pars compacta. *Neurobiology of Aging*, *36*, 3321–3333.

Kamphuis, W., Mamber, C., Moeton, M., Kooijman, L., Sluijs, J. A., Jansen, A. H., … Hol, E. M. (2012). GFAP isoforms in adult mouse brain with a focus on neurogenic astrocytes and reactive astrogliosis in mouse models of Alzheimer disease. *PLoS ONE*, *7*, e42823. https://doi.org/10.1371/journal.pone.0042823

Kamphuis, W., Middeldorp, J., Kooijman, L., Sluijs, J. A., Kooi, E. J., Moeton, M., … Hol, E. M. (2014). Glial fibrillary acidic protein isoform expression in plaque related astrogliosis in Alzheimer's disease. *Neurobiology of Aging*, *35*, 492–510.

Lee, Y. B., Du, S., Rhim, H., Lee, E. B., Markelonis, G. J., & Oh, T. H. (2000). Rapid increase in immunoreactivity to GFAP in astrocytes in vitro induced by acidic pH is mediated by calcium influx and calpain I. *Brain Research*, *864*, 220–229.

Lewerenz, J., Ates, G., Methner, A., Conrad, M., & Maher, P. (2018). Oxytosis/ferroptosis—(Re-) emerging roles for oxidative stress-dependent non-apoptotic cell death in diseases of the central nervous system. *Frontiers in Neuroscience*, *12*(Art), 214.

Liguori, I., Russo, G., Curcio, F., Bulli, G., Aran, L., Della-Morte, D., … Abete, P. (2018). Oxidative stress, aging, and diseases. *Clinical Interventions in Aging*, *13*, 757–772.

Liu, C., Liang, M. C., & Soong, T. W. (2019). Nitric oxide, iron and neurodegeneration. *Frontiers in Neuroscience*, *13*, 114.

Liu, Y., Zhou, Q., Tang, M., Fu, N., Shao, W., Zhang, S., … Zhou, J. (2015). Upregulation of alphaB-crystallin expression in the substantia nigra of patients with Parkinson's disease. *Neurobiology of Aging*, *36*, 1686–1691.

Mena, M. A., de Bernardo, S., Casarejos, M. J., Canals, S., & Rodríguez-Martín, E. (2002). The role of astroglia on the survival of dopamine neurons. *Molecular Neurobiology*, *25*, 245–263.

Monzani, E., Nicolis, S., Dell'Acqua, S., Capucciati, A., Bacchella, C., Zucca, F. A., … Casella, L. (2019). Dopamine, oxidative stress and protein-quinone modifications in Parkinson's and other neurodegenerative diseases. *Angewandte Chemie International Edition English*, *58*, 6512–6527.

Mouser, P. E., Head, E., Ha, K. H., & Rohn, T. T. (2006). Caspase-mediated cleavage of glial fibrillary acidic protein within degenerating astrocytes of the Alzheimer's disease brain. *The American Journal of Pathology*, *168*, 936–946.

Murphy, T. H., Yu, J., Ng, R., Johnson, D. A., Shen, H., Honey, C. R., & Johnson, J. A. (2001). Preferential expression of antioxidant response element mediated gene expression in astrocytes. *Journal of Neurochemistry*, *76*, 1670–1678.

Mythri, R. B., Venkateshappa, C., Harish, G., Mahadevan, A., Muthane, U. B., Yasha, T. C., … Shankar, S. K. (2011). Evaluation of markers of oxidative stress, antioxidant function and astrocytic proliferation in the striatum and frontal cortex of Parkinson's disease brains. *Neurochemical Research*, *36*, 1452–1463.

Mytilineou, C., Kramer, B. C., & Yabut, J. A. (2002). Glutathione depletion and oxidative stress. *Parkinsonism and Related Disorders*, *8*, 385–387.

Naskar, A., Mahadevan, A., Philip, M., & Alladi, P. A. (2019). Aging mildly affects dendritic arborisation and synaptic protein expression in human

substantia nigra pars compacta. *Journal of Chemical Neuroanatomy*, *97*, 57–65.

Pabba, M., Scifo, E., Kapadia, F., Nikolova, Y. S., Ma, T., Mechawar, N., … Sibille, E. (2017). Resilient protein co-expression network in male orbitofrontal cortex layer 2/3 during human aging. *Neurobiology of Aging*, *58*, 180–190.

Paslawski, W., Zareba-Paslawska, J., Zhang, X., Hölz, K., Wadensten, H., Shariatgorji, M., … Svenningsson, P. (2019). α-synuclein–lipoprotein interactions and elevated ApoE level in cerebrospinal fluid from Parkinson's disease patients. *Proceedings of the National Academy of Sciences of the United States of America*, *116*, 15226–15235.

Paxinos, G., & Watson, C. (2005). *The rat brain in stereotaxic coordinates* (5th ed.). San Diego, CA: Academic Press.

Peng, C., Gathagan, R. J., Covell, D. J., Medellin, C., Stieber, A., Robinson, J. L., … Lee, V. M. Y. (2018). Cellular milieu imparts distinct pathological α-synuclein strains in α-synucleinopathies. *Nature*, *557*, 558–563.

Perez-Riverol, Y., Csordas, A., Bai, J., Bernal-Llinares, M., Hewapathirana, S., Kundu, D. J., … Vizcaíno, J. A. (2019). The PRIDE database and related tools and resources in 2019: Improving support for quantification data. *Nucleic Acids Research*, *47*(D1), D442–D450. (PubMed ID: 30395289).

Perng, M. D., Wen, S. F., Gibbon, T., Middeldorp, J., Sluijs, J., Hol, E. M., & Quinlan, R. A. (2008). Glial fibrillary acidic protein filaments can tolerate the incorporation of assembly-compromised GFAP-delta, but with consequences for filament organization and alphaB-crystallin association. *Molecular Biology of the Cell*, *19*, 4521–4533.

Rajagopal, S., Deb, I., Poddar, R., & Paul, S. (2016). Aging is associated with dimerization and inactivation of the brain-enriched tyrosine phosphatase STEP. *Neurobiology of Aging*, *41*, 25–38.

Rashid, M. A., Haque, M., & Akbar, M. (2016). Detoxification of carbonyl compounds by carbonyl reductase in neurodegeneration. *Advances in Neurobiology*, *12*, 355–365.

Reeve, A., Simcox, E., & Turnbull, D. (2014). Ageing and Parkinson's disease: Why is advancing age the biggest risk factor? *Ageing Research Reviews*, *14*, 19–30.

Roostaee, A., Beaudoin, S., Staskevicius, A., & Roucou, X. (2013). Aggregation and neurotoxicity of recombinant α-synuclein aggregates initiated by dimerization. *Molecular Neurodegeneration*, *8*, 5. https://doi.org/10.1186/1750-1326-8-5

Salminen, L. E., & Paul, R. H. (2014). Oxidative stress and genetic markers of suboptimal antioxidant defense in the aging brain: A theoretical review. *Reviews in the Neurosciences*, *25*, 805–819.

Sanchez, H. L., Silva, L. B., Portiansky, E. L., Herenu, C. B., Goya, R. G., & Zuccolilli, G. O. (2008). Dopaminergic mesencephalic systems and behavioral performance in very old rats. *Neuroscience*, *154*, 1598–1606.

Segura-Aguilar, J., Paris, I., Muñoz, P., Ferrari, E., Zecca, L., & Zucca, F. A. (2014). Protective and toxic roles of dopamine in Parkinson's disease. *Journal of Neurochemistry*, *129*, 898–915.

Sengupta, P. (2013). The laboratory rat: Relating its age with human's. *International Journal of Preventative Medicine*, *4*, 624–630.

Si, Q., Sun, S., & Gu, Y. (2017). A278C mutation of dihydropteridine reductase decreases autophagy via mTOR signaling. *Acta Biochimica et Biophysica Sinica*, *49*, 706–712.

Siddiqi, Z., Kemper, T. L., & Killiany, R. (1999). Age-related neuronal loss from the substantia nigra-pars compacta and ventral tegmental area of the rhesus monkey. *Journal of Neuropathology & Experimental Neurology*, *58*, 959–971.

Sidransky, E., & Lopez, G. (2012). The link between the GBA gene and parkinsonism. *Lancet Neurology*, *11*, 986–998.

Šoltić, D., Shorrock, H. K., Allardyce, H., Wilson, E. L., Holt, I., Synowsky, S. A., … Fuller, H. R. (2019). Lamin A/C dysregulation contributes to cardiac pathology in a mouse model of severe spinal muscular atrophy. *Human Molecular Genetics*. https://doi.org/10.1093/hmg/ddz195. [Epub ahead of print].

Sun, F., Deng, Y., Han, X., Liu, Q., Zhang, P., Manzoor, R., & Ma, H. (2019). A secret that underlies Parkinson's disease: The damaging cycle. *Neurochemistry International*, *129*, 104484.

Szklarczyk, D., Morris, J. H., Cook, H., Kuhn, M., Wyder, S., Simonovic, M., … von Mering, C. (2017). The STRING database in 2017: Quality-controlled protein–protein association networks, made broadly accessible. *Nucleic Acids Research*, *45*, D362–D368.

Van Den Eeden, S. K., Tanner, C. M., Bernstein, A. L., Fross, R. D., Leimpeter, A., Bloch, D. A., & Nelson, L. M. (2003). Incidence of Parkinson's disease: Variation by age, gender, and race/ethnicity. *American Journal of Epidemiology*, *157*, 1015–1022.

Vernadakis, A. (1988). Neuron-glia interrelations. *International Reviews of Neurobiology*, *30*, 149–224.

Vila, M. (2019). Neuromelanin, aging, and neuronal vulnerability in Parkinson's disease. *Movement Disorders*. https://doi.org/10.1002/mds.27776. [Epub ahead of print].

Walker, L. C. (2018). Sabotage by the brain's supporting cells. *Nature*, *557*, 499–500.

Winkler, C., Sauer, H., Lee, C. S., & Björklund, A. (1996). Short-term GDNF treatment provides long-term rescue of lesioned nigral dopaminergic neurons in a rat model of Parkinson's disease. *Journal of Neuroscience*, *16*, 7206–7215.

Wojtunik-Kulesza, K., Oniszczuk, A., & Waksmundzka-Hajnos, M. (2019). An attempt to elucidate the role of iron and zinc ions in development of Alzheimer's and Parkinson's diseases. *Biomedicine and Pharmacotherapy*, *111*, 1277–1289.

Xu, F., Sudo, Y., Sanechika, S., Yamashita, J., Shimaguchi, S., Honda, S., … Ichinose, H. (2014). Disturbed biopterin and folate metabolism in the Qdpr-deficient mouse. *FEBS Letters*, *588*, 3924–3931.

Zhai, S., Tanimura, A., Graves, S. M., Shen, W., & Surmeier, D. J. (2018). Striatal synapses, circuits, and Parkinson's disease. *Current Opinions in Neurobiology*, *48*, 9–16.

Zhang, S., Wang, R., & Wang, G. (2019). Impact of dopamine oxidation on dopaminergic neurodegeneration. *ACS Chemical Neuroscience*, *10*, 945–953.

Zhang, X., Gao, F., Wang, D., Li, C., Fu, Y., He, W., & Zhang, J. (2018). Tau pathology in Parkinson's Disease. *Frontiers in Neurology*, *9*, 809.

Zhang, Z., Zoltewicz, J. S., Mondello, S., Newsom, K. J., Yang, Z., Yang, B., … Wang, K. K. (2014). Human traumatic brain injury induces autoantibody response against glial fibrillary acidic protein and its breakdown products. *PLoS ONE*, *9*, e92698. https://doi.org/10.1371/journal.pone.0092698

SUPPORTING INFORMATION

Additional Supporting Information may be found online in the Supporting Information section.

TABLES S1-S8 This document contains supplementary tables S1-S8
This document contains Supplementary Material
Transparent Peer Review Report
Transparent Science Questionnaire for Authors

How to cite this article: Gómez-Gálvez Y, Fuller HR, Synowsky S, Shirran SL, Gates MA. Quantitative proteomic profiling of the rat substantia nigra places glial fibrillary acidic protein at the hub of proteins dysregulated during aging: Implications for idiopathic Parkinson's disease. *J Neuro Res*. 2020;00:1–16. https://doi.org/10.1002/jnr.24622